

Synthesis, Spectroscopy, and Semiempirical Study of a Novel Porphyrin – Flavin Dyad

Dominik T. Hermann,^[b] Anne Christina Schindler,^[b] Kurt Polborn,^[b] Rudolf Gompper,^[b, †] Susanne Stark,^[a, c] Andreas B. J. Parusel,^[a, c, d] Gottfried Grabner,^[a] and Gottfried Köhler*^[a, c]

Abstract: A new synthetic methodology for the preparation of donor–bridge–acceptor compounds incorporating a porphyrin donor and an all-aromatic oligo(diazaphenylene) bridge is introduced. This approach allows the controlled preparation of photosynthetic model compounds with well-defined spacer structure and properties. The synthesis of the porphyrin–flavin dyads **1a–c** is described to exemplify the strategy. This type of structure has a number of interesting spectroscopic and photophysical properties. The aromatic

bridge results in a well-defined donor–acceptor distance; it can favor conjugation and at the same time be nonabsorbing in the visible and near-UV range. The choice of a flavin as the acceptor unit opens the way to a spectroscopic study by excitation of the acceptor in addition to the usual porphyrin donor excitation. Based on these premises, a

Keywords: electron transfer • flavins • fluorescence spectroscopy • photosynthesis • porphyrinoids

spectroscopic, photophysical and semiempirical study of the dyad **1a** has been performed in three solvents of varying polarity. The results demonstrate energy transfer from flavin to porphyrin with unit efficiency at high solvent polarity. In solvents of medium polarity an additional internal conversion pathway is opened following excitation of the flavin moiety. Spectroscopic, cyclovoltammetric, and semiempirical results all suggest that this pathway involves the intermediate population of a short-lived charge-separated state.

Introduction

Photoinduced electron and energy transfer are fundamental processes in biology, chemistry, and materials science.^[1] The first steps in natural photosynthesis involve collection of light energy and energy transfer to the photosynthetic reaction center^[2] followed by a sequence of electron-transfer steps between porphyrin units and from porphyrins to quinones. In

this multistep electron-transfer strategy, charge separation across membranes with a quantum yield near unity is obtained. At each intermediate step the forward reaction has to be faster than back electron transfer. It became a challenge to design synthetic electron-transfer systems, consisting of an electron donor and an acceptor unit separated by a spacer moiety, which are able to mimic the natural processes.^[3] Many of these biomimetic compounds are based on the naturally occurring constituents of the photosynthetic reaction center, namely, porphyrins, which act as the electron donor in electron-transfer systems^[4] or as the energy acceptor in energy-transfer systems,^[5] and a quinone moiety, the terminal electron acceptor in the natural electron-transfer sequence. Quinones have a high electron affinity and an absorption spectrum in the far UV not overlapping with the visible and near-UV spectrum of the porphyrin. Several such model systems have been prepared in recent years and have been studied by various spectroscopic techniques.

The spacer separating two chromophores with different redox properties, which can also be a single bond, is of particular importance. In various publications a rigid structure has been favored,^[6] since only a well-defined geometry allows the interpretation of parameters like the distance between donor and acceptor subunits or their mutual orientation. $\sigma^{[6a-f]}$

[a] Prof. Dr. G. Köhler, Mag. S. Stark, Dr. A. B. J. Parusel, Dr. G. Grabner
Institute for Theoretical Chemistry and Radiation Chemistry
University of Vienna, Althanstrasse 14
A-1090 Vienna (Austria)
Fax: (+43) 1-31336-790
E-mail: gottfried.koehler@univie.ac.at

[b] Dipl.-Chem. D. T. Hermann, Dr. A. C. Schindler, Dr. K. Polborn,
Prof. Dr. R. Gompper^[†]
Institut für Organische Chemie, Universität München
Butenandtstrasse 5–13, D-81377 München (Germany)
Fax: (+49) 89-2180-7640

[c] Austrian Society for Aerospace Medicine–Institute for Space Biophysics
Lustkandlgasse 52, A-1090 Vienna (Austria)

[d] On leave to NASA Ames Research Center, Moffett Field, CA 94035 (USA)

[†] Prof. Gompper died on March 28th, 1999.

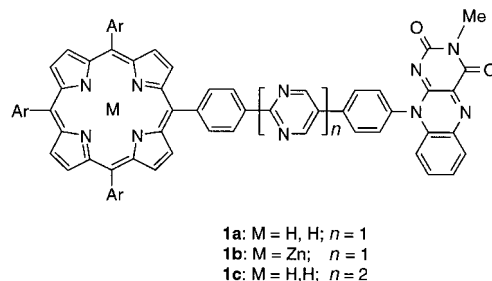
and π spacers^[7] as well as combinations^[6g–i] of both have been designed. Pure aromatic spacers like oligophenylenes or similar structures have, however, rarely been described,^[7c, 8] in spite of several obvious advantages. In addition to their rigid structure they have excellent chemical stability. The length of such a bridge can easily be controlled. It is transparent in the visible and near-UV spectroscopic region and its absorption does not interfere with that of the porphyrin, although overlap with that of small quinones might occur. π -Conjugation of such a spacer depends essentially on its molecular structure and could thus either facilitate or hinder electron transfer over the bridge.

In recent publications the synthesis of oligo(diazaphenylenes) was described by some of us as a strategy for the preparation of tailor-made heteroaromatics displaying fluorescence and nonlinear optical properties.^[9] From readily available vinamidinium salts and amidines or *N,N,N'*-tris(trimethylsilyl)amidines a homologous series of oligo(pyrimidinylphenylenes) could be synthesized in steps with high yield and purity. Symmetrical as well as unsymmetrical systems with a variety of substituents were investigated. The objective of our present work was to apply this synthetic “Lego” methodology to the synthesis of porphyrinyl donor–acceptor systems. The idea was to connect donor and acceptor groups with thermally and photochemically stable pyrimidine and phenylene moieties and finally to arrive at highly rigid photosynthetic model compounds.

In order to avoid spectroscopic overlap of the absorption of the acceptor with that of the spacer and of the donor a flavin^[10] moiety was selected as a possible acceptor entity.

Abstract in German: In dieser Arbeit wird ein neues Konzept zur Herstellung von Donor/Brücke/Akzeptor-Verbindungen vorgestellt. Dabei wird der Porphyrin-Donor mit dem Akzeptor ausschließlich über aromatische Oligo(diazaphenylene) verbunden. Eine derartige Verknüpfung erlaubt eine geometriedefinierte Anordnung der Chromophorkomponenten dieser Photosynthese-Modellverbindungen. Das Konzept wird anhand der Synthese der Porphyrin–Flavin-Dyaden **1a–c** beschrieben. Der vorgestellte Strukturtyp bietet eine Reihe interessanter spektroskopischer und photophysikalischer Eigenschaften. Die Verknüpfung über aromatische Brücken führt zu einem definierten Donor–Akzeptor-Abstand; sie begünstigt die Konjugation ohne die Absorption im sichtbaren und nahen UV-Bereich zu erhöhen. Die Wahl des Flavins als Akzeptoreinheit erlaubt die spektroskopische Untersuchung durch Anregung des Akzeptors neben der sonst üblichen Porphyrin-Donor-Anregung. Auf dieser Grundlage wurden spektroskopische, photophysikalische und semiempirische Untersuchungen in drei Solventien unterschiedlicher Polarität ausgeführt. Die Ergebnisse zeigen einen vollständigen Energietransfer von der Flavineinheit auf das Porphyrin bei hoher Solvenspolarität. In einem Lösungsmittel mittlerer Polarität öffnet sich nach erfolgter Flavinanregung ein weiterer Zerfallsweg. Sowohl die photophysikalischen und cyclovoltammetrischen Messungen als auch die semiempirischen Berechnungen weisen auf die Besetzung eines kurzlebigen ladungstrennten Zwischenzustandes hin.

Flavin coenzymes are prosthetic groups in some redox proteins.^[11] As catalysts (flavodoxins) they take part in electron- and hydrogen-transfer reactions as well as in the activation of oxygen.^[12] Unlike, for example, NADH, flavin can participate in one- as well as two-electron transfer reactions.^[13] In order to demonstrate the synthetic strategy and to investigate the light-harvesting properties of porphyrin–flavin systems, we have synthesized the dyads **1a–c**. To

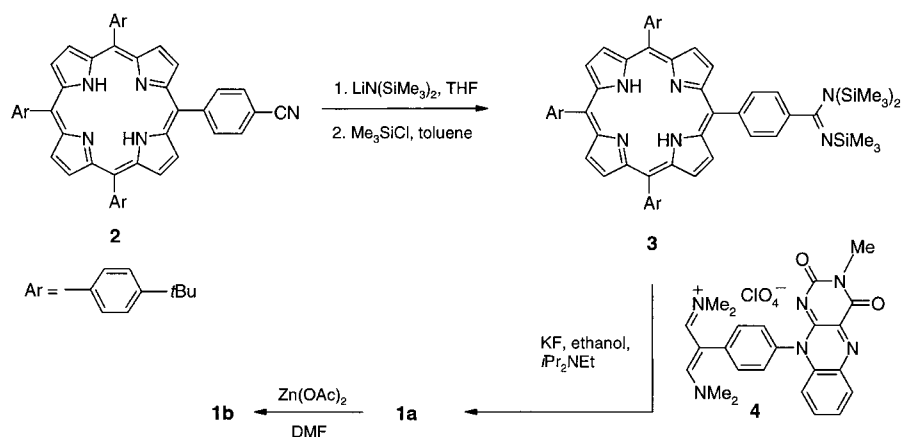


the best of our knowledge only three porphyrin–flavin dyads have been synthesized up to now, which, however, lack the required rigid spacer geometry.^[14] Furthermore, some results on noncovalently linked systems are known.^[15] The electrochemical, spectroscopic, and photophysical properties of dyad **1a** were then examined in various solvents with emphasis on energy- and electron-transfer processes between the two moieties. The results of this study are discussed with respect to semiempirical calculations performed on the same dyad.

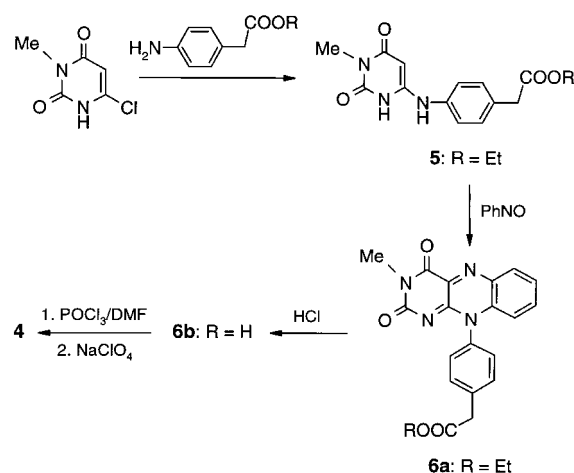
Results and Discussion

1. Synthesis: The synthesis of pyrimidines from amidines and vinamidinium salts has proved to be an excellent method for the preparation of rigid rods of the oligophenyl type.^[9] This method has a number of advantages. Amidines and vinamidinium salts are readily available with virtually no limitations regarding possible substituents.^[9, 16] Pyrimidine rings can be added step by step to get a homologous series of donor/acceptor systems with a controlled spacer length. In contrast to aryl–aryl coupling methods (Suzuki, Stille, Kumada) the “pyrimidine approach” avoids the use of metal catalysts. Thus, the conceivable insertion of metal ions like nickel or copper into the porphyrin ring is avoided.

Using our standard procedure^[9a] the porphyrin–flavin dyad **1a** was obtained from the persilylated porphyrinyl amidine **3** and the flavinyl–vinamidinium salt **4**. The required cyanoporphyrin **2** was prepared from *p*-cyanobenzaldehyde, *p*-tert-butylbenzaldehyde and pyrrole using Adler’s method.^[17a] The product was separated from the porphyrin mixture by chromatography on silica gel. Conversion of the cyano into the amidine group by the Pinner synthesis^[17b] (addition of dry HCl to the mixture of the nitrile and alcohol and subsequent aminolysis of the imidate with NH₃) proved impossible because of the low solubility of **2** in alcohol. However, **2** could be converted into **3** with lithium bis(trimethylsilyl)amide/chlorotrimethylsilane (cf. refs. [9, 18]); **3** was then condensed with **4** in a one-pot reaction. The incorporation of zinc by standard methods^[19] yielded **1b** (Scheme 1).

Scheme 1. Synthesis of model compounds **1a** and **1b**.

The synthesis of the flavin **4** starts from 4-chloro-1-methyluracil^[20] (Scheme 2). Its reaction with *p*-aminophenylacetic acid ester in *N,N*-dimethylaniline and acetic acid gave **5** in 83 % yield. The flavin **6a** was formed from **5** with

Scheme 2. Synthesis of flavinyl-vinamidinium salt **4**.

nitrosobenzene in a mixture of acetic acid and acetic anhydride. Hydrolysis of **6a** with hydrochloric acid gave rise to **6b**. (The direct condensation^[21] of the free acid of **5** ($\text{R} = \text{H}$) with nitrosobenzene to give **6b** failed in our hands.) Finally, the flavinyl-vinamidinium salt **4** was prepared by the Vilsmeier-Haack-Arnold reaction from **6b** with *N,N*-dimethylformamide and phosphoryl chloride.

Crystals of the vinamidinium salt **4** suitable for single-crystal X-ray diffraction were obtained by diffusion of ether into a solution of **4** in acetonitrile. The molecular structure^[22] is illustrated in Figure 1. The vinamidinium moiety exhibits the typical W-form of a cyanine system.^[23] The twist angle of the central phenylene ring against the flavin moiety is 77.3° and that against the cyanine system 87.7° . Thus, the flavin and the cyanine systems are almost coplanar.

The compounds **7** and **8** were required as reference compounds for the photophysical investigation. The unsubstituted porphyrin **7** was prepared under standard conditions from pyrrole and *p*-tert-butylbenzaldehyde. Using a simple

pyrimidine synthesis, the flavin **8** was obtained from the flavinyl-vinamidinium salt **4** and acetamidine.

For future studies of the influence of the donor/acceptor distance in **1**, we have enlarged the spacer by incorporation of a further pyrimidine unit. Condensation of the 2-cyanovinamidinium salt **9**^[24] with the amidine **3** formed from **2** gave the 5-cyanopyrimidinyl porphyrin **10** in 73 %

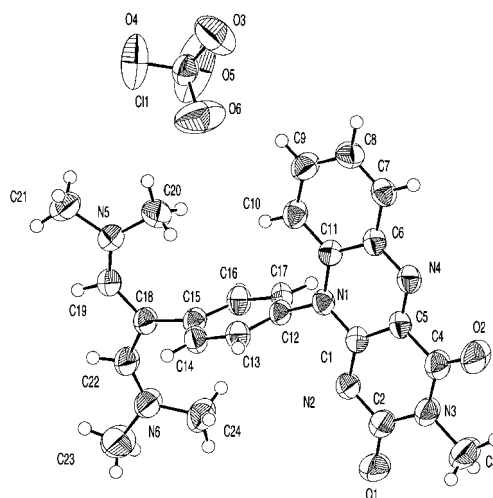
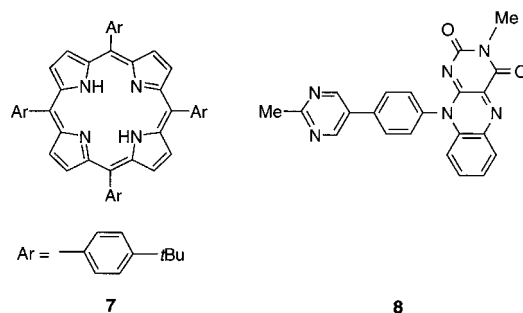
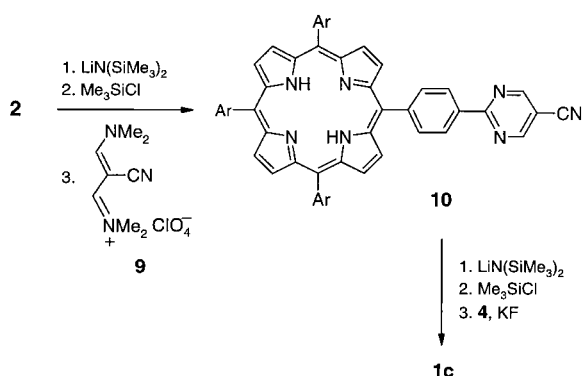


Figure 1. ZORTEP plot of the vinamidinium salt **4**. Selected bond length [pm] and bond angles $^\circ$: N1-C12 145.7(5), C15-C18 149.4(5), C18-C19 140.2(5), C18-C22 139.0(6), C19-N5 131.1(5), C22-N6 130.5(5); C14-C15-C18 117.5(3), C16-C15-C18 124.1(4), C19-C18-C22 111.6(3), N5-C19-C18 132.3(4), N6-C22-C18 132.2(4).



yield (Scheme 3). Application of the reaction sequence displayed in Scheme 1 led to the flavinyl porphyrin **1c**, which is extended by one pyrimidine unit as compared with **1a**.

2. Cyclic voltammetry and estimation of energy levels: Cyclic voltammetric studies on the porphyrin-flavin dyad **1a** were performed in methylene chloride as solvent. They revealed reversible waves indicating oxidation potentials at +0.82 and +1.15 V, relative to ferrocene as reference redox system. Both half-wave potentials are in good agreement with that of the

Scheme 3. Synthesis of model compound **1c**.

first and second oxidation steps of the parent porphyrin **7**. For this compound two oxidation waves with half-wave potentials at +0.81 and 1.13 V were found under the same conditions. The first and second reduction potentials appear at –0.74 and –1.29 V. The first one corresponds to the reduction of the flavin, that is, $\text{Fl}_{\text{ox}}/\text{Fl}^-$ (–0.73 V was found previously^[14a]), and the second one to the first reduction potential of the porphyrin ($\text{PH}_2/\text{PH}_2^{\cdot-}$).^[14a]

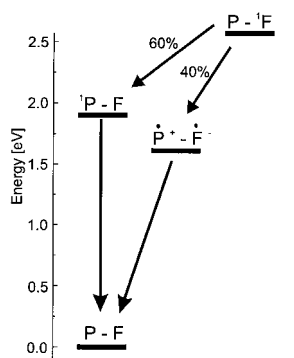
The energy of the charge-separated ion pair state, $E(\text{IP})$, can be estimated from the respective oxidation and reduction potentials according to Equations (1a, 1b),^[15] which also account for variations in solvent polarity. E_{ox} and E_{red} are

$$E(\text{IP}) = E_{\text{ox}} - E_{\text{red}} + \delta G_{\text{s}} \quad (1a)$$

$$\delta G_{\text{s}} = \left(\frac{e^2}{2} \right) \left(\frac{1}{r_{\text{D}}} + \frac{1}{r_{\text{A}}} \right) \left(\frac{1}{4\pi\epsilon_0\epsilon} - \frac{1}{4\pi\epsilon_0\epsilon_{\text{r}}} \right) - \frac{e^2}{4\pi\epsilon_0\epsilon R_{\text{DA}}} \quad (1b)$$

the oxidation and reduction potentials of the donor and acceptor, respectively; r_{D} and r_{A} are the effective radii of the donor cation and acceptor anion, estimated to be 4.3 (porphyrin cation) and 4.4 Å (flavin anion), respectively, and ϵ_{r} (9.08) and ϵ (7.56) are the dielectric constants of methylene chloride and tetrahydrofuran. The distance separating the donor and acceptor subunits (R_{DA}) was estimated to be 19.1 Å (see below). From these values, ion-pair state energies of 1.56 eV for solutions in methylene chloride and of 1.52 eV for solutions in tetrahydrofuran are deduced.

In Scheme 4 the energy level $E(\text{IP})$ is compared with the spectroscopic energy levels of the respective excited S_1 states, as determined from the arithmetic means of the energies of

Scheme 4. Transient states of dyad **1a** and their relevant interconversion pathways.

the corresponding (0,0) transitions of the fluorescence absorption bands of the flavin and porphyrin subunits. A value of 1.90 eV is obtained for the S_1 state of the porphyrin and a value of 2.59 eV for that of the flavin subunit. Although these estimates have rather large uncertainties, the charge-separated state is located well below the lowest excited state of the flavin but also below that of the porphyrin subunits.

3. Semiempirical calculations

3.1. Ground-state properties: The center-to-center distance between the donor and the acceptor in dyad **1a** is 19.1 Å. Its dipole moment is oriented parallel to the flavin unit in the center of the spacer bridge, directed from the homoaromatic subunits towards the heteroaromatic moiety within the flavin unit, and has a magnitude of 6.4 D. The total energy of the optimum geometry becomes 489.6 kcal mol^{–1}. The three phenyl rings attached to the porphyrin unit are twisted by 62–65° relative to the porphyrin plane. Weak electronic coupling between the phenyl groups and the porphyrin moiety accounts for a small increase in total energy (0.7 kcal mol^{–1}) and an increase in the bond length (from 1.47 to 1.5 Å) when the orientation of the three phenyls is perpendicular to the porphyrin plane. Similar results are found for rotation about the two single bonds between the aryl groups of the spacer unit: all aryl rings are slightly twisted relative to each other but diverge significantly from orthogonality. The dihedral angle between the porphyrin ring and the first phenyl ring of the spacer becomes 63.3°, similar to that between the flavin moiety and the last phenyl ring (66.3°). Both dihedral angles between the pyrimidine and the two phenyl rings are near 37°. In both cases the orthogonal arrangement is about 1.2 kcal mol^{–1} higher in energy, whereas a planar orientation is only 0.5 kcal mol^{–1} higher in energy for the less sterically hindered bond but 1.3 kcal mol^{–1} higher for the second, biphenyl-like bond. The optimum arrangement results in a nearly orthogonal orientation between the flavin and porphyrin planes. A more detailed analysis of the ground state geometry was given previously.^[25]

3.2. Molecular orbital analysis: The energies (Figure 2a) and a visualization of the frontier orbitals (Figure 2b) of the tetraphenylporphyrin (**P**) and flavin (**F**) subunits as well as of the dyad **1a** are presented in Figure 2 and Table 1. Most of the important orbitals of dyad **1a** can be related to the MOs of the single components. The HOMO – 1, HOMO, LUMO + 1, and LUMO + 2 of dyad **1a** are localized on the porphyrin moiety and correspond to the orbitals of the porphyrin. The energies of these four orbitals remain almost unchanged when the spacer and flavin subunit are attached to the porphyrin, that is, their character is not strongly affected in the dyad. These orbitals correspond to the four frontier orbitals according to the Gouterman four-orbital model^[26] for porphyrins. The HOMO – 2 represents the highest occupied molecular orbital of the acceptor subunit, but with large contributions from orbitals localized on the spacer. Occupied orbitals of the spacer and of the flavin subunit are thus in a similar energy range and can combine effectively. This explains the high degree of conjugation of the aromatic

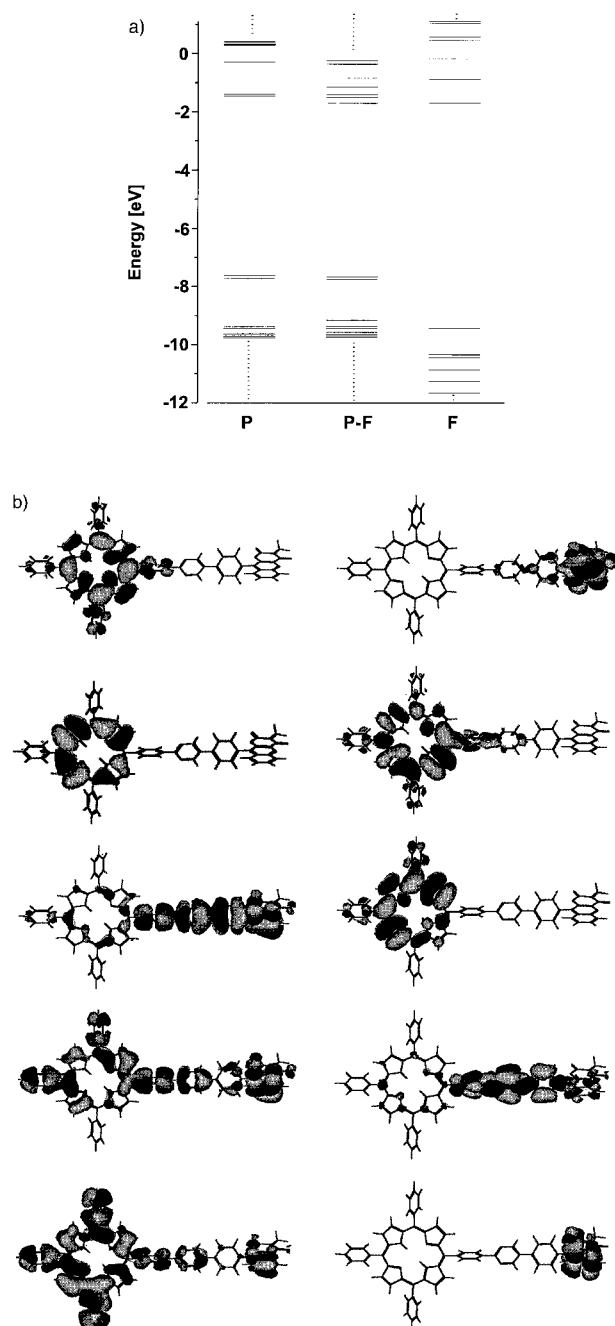


Figure 2. a) Orbital energy (eV) of the frontier orbitals of the tetraphenylporphyrin (**P**), complete dyad (**P-F**), and the flavin (**F**) system; b) visualization of the decisive occupied (left) and unoccupied (right) MO's of the **P-F** dyad (HOMO and LUMO at the top to HOMO - 4 and LUMO + 4 at the bottom).

Table 1. Orbital energies (eV) of the frontier orbitals of the tetraphenylporphyrin (**P**), the complete dyad (**P-F**), and the flavin (**F**) system.

	HOMO - 8	HOMO - 7	HOMO - 6	HOMO - 5	HOMO - 4	HOMO - 3	HOMO - 2	HOMO - 1	HOMO
P	-9.764	-9.727	-9.679	-9.670	-9.631	-9.448	-9.384	-7.727	-7.625
P-F	-9.748	-9.702	-9.667	-9.582	-9.445	-9.382	-9.170	-7.755	-7.675
F	-13.223	-12.737	-12.144	-11.669	-11.263	-10.87	-10.451	-10.356	-9.441
	LUMO	LUMO + 1	LUMO + 2	LUMO + 3	LUMO + 4	LUMO + 5	LUMO + 6		
P	-1.464	-1.404	0.305	0.287	0.306	0.327	0.401		
P-F	-1.720	-1.513	-1.431	-1.161	-0.834	-0.376	-0.26		
F	-1.713	-0.886	-0.199	0.449	0.568	1.037	1.098		

bridge.^[25] Both the HOMO - 3 and HOMO - 4 are of porphyrin character with significant extension to the spacer and even the acceptor subunit. This delocalization accounts for efficient conjugation throughout the whole system. All occupied orbitals above HOMO - 15 are considerably delocalized and only the HOMO - 15 is of pure flavin π character.

Unlike the occupied orbitals, the excited orbitals of the spacer contribute only marginally to the lowest unoccupied orbitals of the dyad. The LUMO of dyad **1a** corresponds to the LUMO of the flavin subunit with only small contributions from the attached spacer unit. LUMO + 4 is completely localized on the flavin moiety without significant contributions from the spacer or the porphyrin. Solely the LUMO + 3 is located exclusively on the spacer unit (Figure 2b) and is thus the only low-lying unoccupied orbital which cannot be directly assigned to the donor or acceptor groups.

This orbital analysis is supported by the energy scheme (Figure 2a) and its comparison with that of the separated donor and acceptor subunits. The energies of the porphyrin orbitals are only slightly changed in the dyad because of their strict localization. In contrast, a marked deviation is found for those localized on the flavin subunit, owing to their extensive delocalization. In summary, occupied orbitals are generally more delocalized than unoccupied ones, but those correlating with porphyrin orbitals are less delocalized than those derived from the flavin moiety.

3.3. Electronic excitation: The properties of the lowest excited singlet states of the dyad are summarized in Table 2. The excitation energy levels of S_1 to S_5 are presented in Figure 3

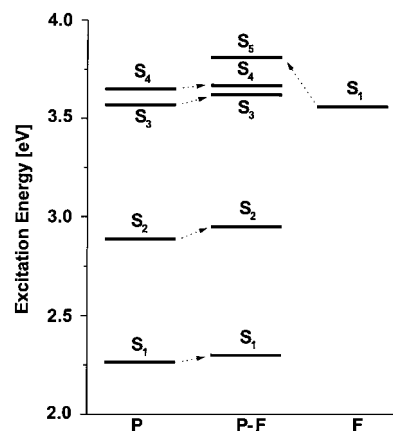


Figure 3. Excitation energy (eV) up to 4.0 eV for the dyad (**P-F**), the tetraphenylporphyrin (**P**), and the flavin (**F**) system.

for both the porphyrin **P** and the flavin **F** subunits, and for the complete **P-F** dyad **1a**. The first four excited states are exclusively of porphyrin character. They result from the combination of excitations promoting an electron from the degenerate orbitals HOMO - 1 and HOMO into LUMO + 1

Table 2. Excitation energies (ΔE in eV), dipole moments (μ in D), oscillator strengths f , and characterization of the first excited singlet and decisive triplet (T_0 and T_{13}) states for the **P–F** dyad. 0–0 corresponds to a HOMO \rightarrow LUMO transition; 1–1 to a HOMO – 1 \rightarrow LUMO + 1 transition and so forth.

		ΔE	μ	f	Character			
T_0	P*–F	1.85	6.5	–	68 %	0–1	27 %	1–2
S_1	P*–F	2.30	6.6	0.011	52 %	0–1	44 %	1–2
S_2	P*–F	2.95	6.6	0.001	50 %	0–2	39 %	1–1
S_3	P*–F	3.62	7.2	1.874	28 %	0–2	32 %	1–1
S_4	P*–F	3.67	7.3	1.652	28 %	0–1	33 %	1–2
S_5	P–F*	3.81	29.3	0.180	42 %	2–0	40 %	3–0
S_6	P–S*–F	4.40	12.9	0.356	31 %	2–3	24 %	0–3
S_{12}	P⁺–F[–]	5.23	70.9	0.023	74 %	0–0		
T_{13}	P⁺–F[–]	5.29	60.3	–	56 %	0–0	11 %	4–2

and LUMO + 2. The S_1 and S_2 states have excitation energies of 2.30 and 2.95 eV, respectively, a small oscillator strength of less than 0.01 and a dipole moment of 6.6 D. These excitations can be assigned to the two Q bands of the absorption spectrum. The corresponding first excited state of triplet character is located in vacuo at an energy of 1.85 eV. The next two states, S_3 and S_4 , are found at 3.62 and 3.67 eV, respectively, and have a somewhat larger dipole moment of 7.3 D and a large oscillator strength of 1.7 to 1.9. These transitions are characteristic for the Soret region of the porphyrin spectrum.^[26] As neither the energy nor the electron distribution of the orbitals (Figure 2b) changes significantly upon substitution of the porphyrin, no significant deviation between the free tetraphenylporphyrin and the **P–F** dyad is expected. This is corroborated by the results presented in Figure 3; an increase in excitation energy of less than 0.1 eV is calculated for the **P–F** dyad in comparison to the unsubstituted porphyrin **P**. The computed oscillator strengths, dipole moments, and also the orbital contributions differ only marginally between the two systems investigated.

The fifth excited state S_5 , with an excitation energy of 3.81 eV, is best described as a flavin excited state. In contrast to the porphyrin excited states, excitations of the flavin moiety in the dyad differ notably from the comparable excitations of the free flavin. This can be seen in Figure 3: the excitation energy in the dyad is significantly higher than in the flavin **F**. The initial orbitals HOMO – 2 and HOMO – 3 are additionally stabilized by delocalization over the spacer and the porphyrin unit, whereas the final, excited orbitals are localized on the flavin. This causes an increase of the energy gap between those orbitals and, thus, of the excitation energy, and also a high excited-state dipole moment of 29.3 D, which is much larger than that of the respective flavin excited state (12.7 D).

The next higher excited singlet state, S_6 , with an excitation energy of 4.40 eV, cannot be assigned to any transition located on the porphyrin or flavin subunit. It can be characterized as a mixture of the two transitions HOMO \rightarrow LUMO + 3 and HOMO – 2 \rightarrow LUMO + 3. The occupied orbitals are localized on the porphyrin and the flavin subunits, but the terminal orbital is localized on the spacer group (Figure 2b, Table 2.). Electronic charge density is thus shifted from both the donor and the acceptor moiety to the center of the molecule on the

spacer and an excited state with a comparatively small dipole moment, 12.9 D, results.

An excited state corresponding to electron transfer from the donor to the acceptor is found as S_{12} , with an excitation energy of 5.23 eV. This state is essentially described as the HOMO \rightarrow LUMO one-electron transition. The HOMO is localized on the porphyrin, whereas the accepting LUMO is mainly located on the flavin. The corresponding triplet is found at almost the same energy at 5.29 eV. The small energy gap between the singlet and triplet excited states is characteristic for an electron transfer state. In the case of the charge separated state **P⁺–F[–]**, a huge formal dipole moment of 70.9 D is calculated.

3.4. Energy transfer: The separation between the porphyrin and flavin excited states and the overlap of the fluorescence of the latter with the porphyrin Q bands (see below) enables efficient energy transfer from the flavin to the porphyrin fluorescent state (**P \leftarrow F**), when the flavin subunit is selectively excited (**P–F***). The spectroscopic investigation of the dyad **1a** has confirmed the possibility of a selective excitation of the **P–F*** state and efficient relaxation to the **P*–F** excited state. For efficient energy transfer from the flavin to the porphyrin by a Förster mechanism the transition dipole moments for the two terminating states have to be oriented parallel to each other. The calculated transition dipole moments for the first five excited states as well as the angles between them have been computed for the optimum geometry of the dyad, and the results are presented in Table 3.

Table 3. Transition dipole moment for the five lowest excited states of **P–F** and angle α (°) between the transition dipole moments of the **P–F*** and **P*–F** excited states S_1 to S_4 .

	x	y	z	α
S_1	0.23	0.03	0.05	56
S_2	0.05	–0.01	0.01	56
S_3	1.94	–1.34	0.61	67
S_4	–1.70	–1.50	–0.08	122
S_5	0.53	0.01	–0.51	

In the optimized ground-state structure of the dyad **1a**, the transition dipole moment of the flavin excited state (i.e., the S_5 of the dyad) lies in a plane at an angle of approximately 60° to the plane of the porphyrin ring system. The angle between the transition dipole moments of the excited S_1 and S_2 porphyrin states and that of S_5 is, therefore, also in the vicinity of 60°. The energy for a rotation of the flavin moiety about the connection of the two subunits is below 0.5 kcal mol^{–1} for angles $\leq \pm 40^\circ$ relative to the orthogonal geometry. This allows for sufficient thermal flexibility to ensure efficient coupling of the two transitions located on the two subunits and facilitates energy transfer **P \leftarrow F***. An internal conversion process from the S_5 into the lowest porphyrin excited states by energy transfer can thus be very fast.

3.5. Solvent effects: Solvent effects of a polar environment are estimated by the Onsager model.^[27] Although this model is in

principle not valid for the case of large molecules, like the dyad, for which the dipole moment cannot be considered to be infinitesimally small in comparison to the solvent-excluded volume, it nevertheless allows an estimate of the stabilization energy of the charge-separated state in a polar solvent. As the shape of the investigated dyad **1a** (**P**–**F**) deviates significantly from a sphere, its volume was described by an ellipsoid with axes *a* (long axis), *b*, and *c*.

Solvation energies for the excited states were calculated by two different approaches, bearing in mind solvent influences on absorption spectra on the one hand and on state energies on the other. In the first case, reorientation of the solvent molecules is disregarded. The effect on vertically excited states is calculated accounting for orientation of the dipoles in the ground state and polarization of the medium caused by the increase of the dipole moment upon excitation from μ_i in the ground state to μ_f in the excited states [Eq. (2)],^[28] where ϵ_0 is

$$\Delta E_{\text{solv,partial}} = -\frac{2\mu_i\mu_f}{4\pi\epsilon_0 abc} \left(\frac{\epsilon - 1}{2\epsilon + 1} - \frac{n^2 - 1}{2n^2 + 1} \right) - \frac{2\mu_f^2}{4\pi\epsilon_0 abc} \frac{n^2 - 1}{2n^2 + 1} \quad (2)$$

the universal dielectric constant, ϵ the dielectric permittivity of the solvent, *a*, *b*, and *c* the three axes of the ellipsoid describing the Onsager cavity, and *n* is the refractive index of the solvent. When, in addition, full reorientation of the solvent molecules is allowed for according to the charge distribution in the relaxed excited state, the total solvation energy $\Delta E_{\text{solv,relax}}$ is obtained from Equation (3).^[27]

$$\Delta E_{\text{solv,relax}} = \frac{2\mu^2}{4\pi\epsilon_0 abc} \frac{\epsilon - 1}{2\epsilon + 1} \quad (3)$$

The total energies of excited states in a solvent of given permittivity and refractive index are obtained by adding the respective solvation energy ΔE to the gas-phase transition energies. In order to allow comparison with experiment, the calculations were carried out for tetrahydrofuran as a polar aprotic solvent with $\epsilon = 7.56$ and $n = 1.407$. The values for the radii of the ellipsoid cavity were estimated from the molecular structure to be *a* = 15.4, *b* = 8.8, and *c* = 5.2 Å. The resulting energy state diagram in the solvent THF is shown in Figure 4.

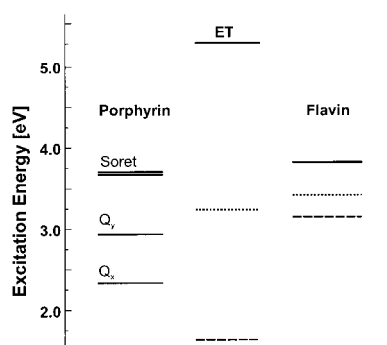


Figure 4. Energy scheme (eV) for the energy of the **P***–**F** (Q and Soret states), **F**–**P***, and **P**⁺–**F**[−] singlet states in vacuo (—) and in tetrahydrofuran unrelaxed (····) and relaxed (----) solvent cage according to the Onsager model.

It has to be mentioned at this point that small changes in the cavity radii cause large shifts in the computed stabilization energy; in particular, the charge-separated state is sensitive to

this parameter owing to its huge formal dipole moment. With this limitation in mind, the study of the solvent effects reveals the reversal of the excited-state progression due to solvent stabilization. The electron-transfer state S_{12} becomes the first excited state, at a total energy of about 1.6 eV. The S_5 flavin-like excited state, with a large dipole moment of more than 29 D, is also significantly stabilized in total energy. Nevertheless, the first **P***–**F** state is lower in total energy than the **P**–**F*** state in the polar environment too. Further computed energies are 1.9 eV for the first porphyrin excited state, 3.2 and 3.3 eV for the Soret bands, and 2.6 eV for the flavin excited state; this latter state thus lies between the Q and Soret absorption bands of the dyad. Efficient energy transfer from the flavin to the porphyrin unit is still possible, too. These results are both in agreement with experiment. The stabilization of the **P**⁺–**F**[−] state allows its population by deactivation of both the **P***–**F** and of the **P**–**F*** state. As discussed in the previous section in connection with the problem of electronic coupling, the **P**–**F*** state is the more likely origin for formation of a charge-separated state.

4. Spectroscopic and photophysical properties

4.1. Absorption spectra: The absorption spectra of the dyad **1a** together with those of the reference compounds, flavin **8** and porphyrin **7**, in a tetrahydrofuran solution are shown in Figure 5. The main contributions of the porphyrin substructure

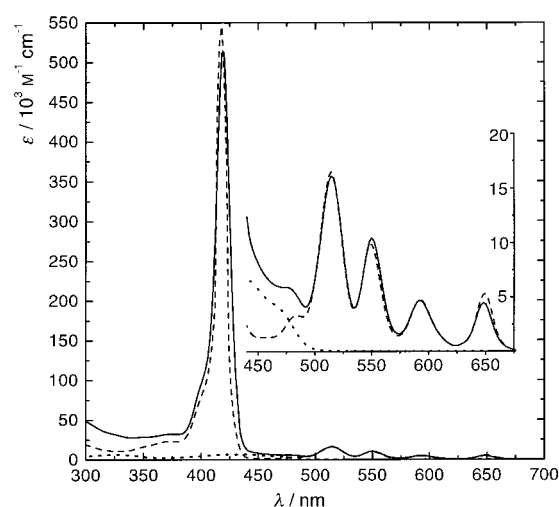


Figure 5. Absorption spectra of the dyad **1a** (—), porphyrin **7** (---), and flavin **8** (····) in tetrahydrofuran as solvent (*T* = 20°C). The Q bands are plotted to an extended scale in the inset.

ture to the absorption spectrum of the dyad are easily recognized: the intense Soret band (B band) appears at about 420 nm and the typical vibronically resolved Q bands (Q_{Y01} , Q_{Y00} , Q_{X01} , Q_{X00}) of a doubly protonated porphyrin are observed in the 470–700 nm wavelength range. The flavin absorption is found in the range between 400 and 490 nm and in the UV below 370 nm, and is also recovered in the spectrum of the dyad. In the far UV around 300 nm, absorption due to the spacer becomes significant.

Details of the absorption spectra (absorption maxima and extinction coefficients) of the dyad and the subunits are compiled in Table 4. The data show small but distinct changes in the spectral parameters between the dyad and the

Table 4. Absorption maxima λ_{max} and extinction coefficients ϵ of the porphyrin–flavin dyad **1a** in tetrahydrofuran (THF) and comparison to flavin **8** and porphyrin **7** (20 °C).

Compound	λ_{max} (nm)		ϵ (M ⁻¹ cm ⁻¹)	
	Flavin (S ₀ ← S ₃ , S ₂ , S ₁)	Porphyrin (Soret band)	Porphyrin (Q bands)	
flavin 8	264	24 300		
	328	4800		
	438	5200		
porphyrin 7		418	545 600	514 16 500
			550	9890
			592	4700
			650	5300
porphyrin–flavin dyad 1a		420	512 500	514 16 100
			550	10 500
			592	4700
			648	4500

individual model compounds; the most significant is a bathochromic shift of 2 nm and a slight broadening of the Soret band in the dyad compared to that of porphyrin **7**. A small solvent shift of the Soret band is observed in the solvents toluene, tetrahydrofuran, and dimethylformamide, in agreement with the variation of the refractive index.

Most importantly, the absorption due to the flavin moiety is well separated from the porphyrin Soret and Q bands; consequently, the flavin moiety can be nearly selectively excited in the wavelength range between 450 and 475 nm. From the absorption spectra of porphyrin **7**, flavin **8**, and the porphyrin–flavin dyad and their small changes it can be estimated that for excitation at 465 nm the flavin subsystem is selectively excited to 78 % in the solvent toluene, to 80 % in tetrahydrofuran, and to 76 % in *N,N*-dimethylformamide. On the other hand, the porphyrin group can be exclusively excited in each one of the Q bands, for example at 517 nm.

4.2. Fluorescence measurements: The normalized fluorescence spectra of the dyad **1a** and of the model compounds in tetrahydrofuran are shown in Figure 6. Spectra of the dyad are given for two excitation wavelengths, 517 nm, where exclusively the porphyrin moiety is excited, and 465 nm, where excitation is predominantly into the flavin subunit. Excitation of porphyrin **7** and of the dyad at 517 nm results in the typical porphyrin emission spectrum showing maxima at 654 and 720 nm that correspond to the Q_{X00}^{*} and Q_{X01}^{*} vibrational bands.^[29] The fluorescence maximum of flavin **8** is located at

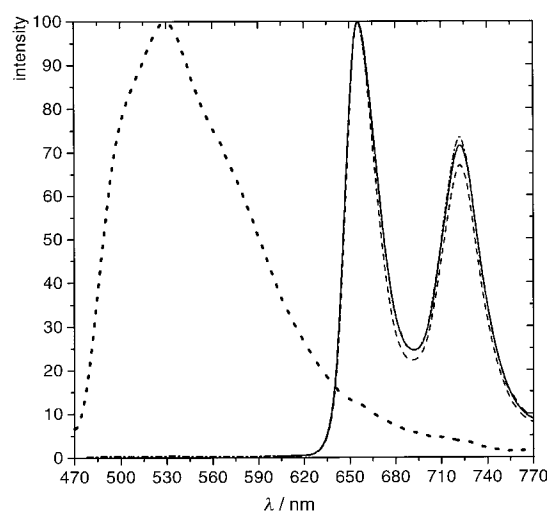


Figure 6. Normalized fluorescence emission spectra of the dyad **1a** for excitation into the porphyrin at 517 nm (—) and the flavin subunit at 465 nm (---), of porphyrin **7** (excitation at 517 nm, ----) and flavin **8** (excitation at 465 nm, ····) in tetrahydrofuran as solvent (*T* = 20 °C). The spectra are normalized to equal height at their maxima.

532 nm. Excitation of the dyad at 465 nm gives only a very low emission in the wavelength range corresponding to the flavin group, but a strong porphyrin fluorescence is also observed. The flavin excited state is thus strongly quenched and relaxes predominantly to the porphyrin excited state. Fluorescence quantum yields Φ_F and fluorescence lifetimes τ_F of dyad **1a** and the two model compounds were measured in toluene, tetrahydrofuran, and *N,N*-dimethylformamide at various excitation wavelengths (see Table 5).

Table 5. Fluorescence quantum yield and lifetime for the dyad **1a** in comparison to flavin **8** and porphyrin **7** in toluene, tetrahydrofuran (THF), and dimethylformamide (DMF), measured at *T* = 20 °C. β defines the yield for the relaxation process from the excited flavin to the fluorescent porphyrin state.

Compound	Φ_F τ_F (ns)						Porphyrin emission					
	toluene		Flavin emission THF		DMF		toluene		THF		DMF	
flavin 8 ^[a]	0.20	3.4	0.13	2.8	0.16	3.3						
porphyrin 7 ^[b]							0.10	11.2	0.13	11.1	0.12	10.4
porphyrin–flavin dyad 1a ^[b]							0.12	11.5	0.15	11.9	0.12	10.2
^[a]	≤ 0.001	–	≤ 0.001	–	≤ 0.001	–	0.09	11.6	0.10	11.1	0.13	10.3
β (± 0.02)							0.68		0.58		1.05	

[a] Excitation of the flavin at 465 nm. [b] Excitation of the porphyrin at 517 nm.

When the porphyrin **7** and the dyad are excited at 517 nm they show equal fluorescence spectra and similar fluorescence lifetimes and quantum yields. The latter are generally slightly higher for the dyad in comparison to the porphyrin model. This indicates that no additional deactivation mechanism is operative when the dyad is excited into the porphyrin substructure.

The fluorescence quantum yields measured for excitation at 465 nm result mainly from excitation of the flavin chromophore but in part also from direct excitation of the porphyrin. The Φ_F values measured at 465 nm are considerably smaller

than those found for the excitation into the Q bands, but this effect depends significantly on the solvent polarity: in solutions in toluene and tetrahydrofuran, the values obtained for excitation at 465 nm are indeed less than those for excitation at 517 nm, but the effect was absent for solutions in the highly polar solvent dimethylformamide. This indicates that the flavin excited state does not quantitatively relax to the porphyrin fluorescent state in toluene and tetrahydrofuran. This internal conversion pathway of the primarily excited state can be characterized by a quantum efficiency, β , the values of which are given in Table 5 for the three solvents used. The data show that approximately 60% of the initially excited flavin state converts to the porphyrin fluorescent state, 40% relaxes nonradiatively and less than 1% decays by fluorescence. By contrast, in the solvent dimethylformamide flavin excitation quantitatively results in porphyrin fluorescence.

A value for the lifetime of the excited flavin in the dyad can be estimated from the measured decrease of its fluorescence quantum yield in solution (Q_f^0) and in the dyad (Q_f) and its fluorescence lifetime (τ_f^0). From the values given in Table 5 a lifetime shorter than 25 ps can be estimated by means of Equation (4). Nonradiative quenching is thus very fast, with a

$$k_{nr} \approx \frac{1}{\tau_f} = \frac{1}{\tau_f^0} \left(\frac{Q_f^0}{Q_f} - 1 \right) \quad (4)$$

rate constant $k_{nr} \geq 4 \times 10^{10} \text{ s}^{-1}$. This rate is smaller than the normal rates for internal conversion processes due to vibronic coupling of the excited states, and fluorescence from the upper state is thus still visible. It is assumed that the conversion from the flavin excited state to the S_1 of porphyrin is due to resonance energy transfer. This process should be rather efficient as fluorescence and absorption of the two terminating states overlap efficiently.

4.3. Nanosecond transient absorption spectroscopy: Solutions in tetrahydrofuran of the dyad **1a** as well as of the porphyrin and flavin model compounds **7** and **8** were subjected to laser flash photolysis at concentrations between $5 \times 10^{-6} \text{ M}$ and 10^{-5} M . The optical parametric oscillator wavelengths $\lambda_1 = 450 \text{ nm}$ and $\lambda_2 = 517 \text{ nm}$ were used to ensure, as far as possible, selective excitation of the flavin and porphyrin moieties of the dyad. Typical ground-state absorbances of the dyad, measured in a 1 cm cell, were $A(\lambda_1) = 0.058$ and $A(\lambda_2) = 0.100$. At λ_1 , the contribution of the porphyrin moiety to the total absorbance was 38%. Excitation of the flavin **8** at λ_1 resulted in barely measurable transient absorbances ($A < 0.001$ at 1 mJ/pulse). Measurable but still very weak transients were observed when the fourth harmonic of the Nd:YAG laser ($\lambda = 266 \text{ nm}$) was chosen for excitation; at this wavelength, the flavin **8** has an intense absorption maximum $\epsilon = 36000 \text{ M}^{-1} \text{ cm}^{-1}$. A broad transient absorption with a maximum around 450 nm and a lifetime of the order of 100 μs could be detected; the absorbance increased with pulse energy in a distinctly nonlinear way. This observation is consistent with the previously reported formation of a flavosemiquinone radical by two-photon ionization of 1,5-dihydroflavin mononucleotide.^[30a] The efficiency of this two-

photon process is noticeably higher when excitation occurs at 266 nm rather than at 450 nm.

Excitation of the porphyrin **7** in THF at λ_2 resulted in the transient difference spectrum shown in Figure 7, featuring a prominent band in the 430–460 nm range and a weaker

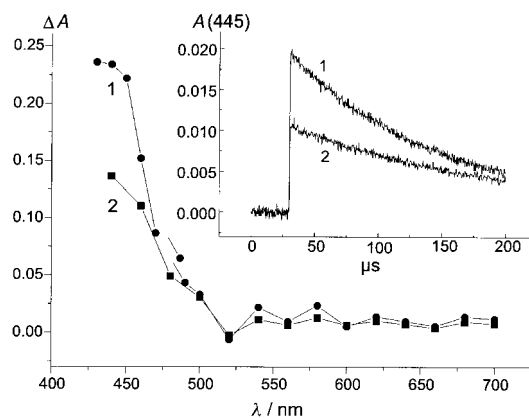


Figure 7. Transient spectra from laser flash photolysis of deoxygenated THF solutions of porphyrin **7**, excited at $\lambda_2 = 517 \text{ nm}$ (spectrum 1, ●) and of the dyad, excited at $\lambda_1 = 450 \text{ nm}$ (spectrum 2, ■). Values of ΔA normalized to unit absorbance at wavelength of excitation. Inset: Time course of absorbance for dyad excited at λ_2 (1) and at λ_1 (2).

absorption tailing towards the red. The lifetime of this transient was of the order of 50 μs in solutions that were deoxygenated by bubbling with N_2 ; its decay was accelerated in the presence of O_2 . The decay kinetics were independent of wavelength between 430 and 700 nm. Assignment of this transient to the triplet-minus-singlet spectrum of **7** is straightforward; similar spectra have been obtained for other porphyrins.^[30b] The dependence of the transient absorbance on laser pulse energy was found to be linear at low pulse energies ($< 0.5 \text{ mJ/pulse}$); a value of $\epsilon(\lambda_m) \times \phi = 18000 \text{ M}^{-1} \text{ cm}^{-1}$ was determined at $\lambda_m = 445 \text{ nm}$.

The transient obtained by photoexcitation of the dyad was spectrally and kinetically very similar to that resulting from the porphyrin **7** for excitation at λ_1 and λ_2 alike: the transient behavior of the dyad is dominated by the triplet state of the porphyrin moiety no matter whether the porphyrin or the flavin moiety is excited. In order to get a more detailed picture, we measured the pulse energy dependence of the transient absorption at three selected wavelengths, 445, 570, and 670 nm, for both excitation conditions. The measuring wavelengths were chosen for the following reasons: 445 and 570 nm for a high ratio of triplet absorption to ground-state depletion, and 670 nm as a representative wavelength where the potential formation of a porphyrin radical cation originating from long-lived charge separation in the dyad would show up.^[3] The dependence of absorbance on pulse energy read at pulse end was in all cases linear up to 0.5 mJ/pulse, allowing the determination of $\epsilon(\lambda_m) \times \phi$ (see Experimental Section); the results are shown in Table 6. Two conclusions can be drawn based on these data: first, excitation of the porphyrin moiety of the dyad generates the porphyrin triplet with the same quantum yield as from the free porphyrin; second, the ratios of $\epsilon(\lambda_m) \times \phi$ values for excitation of the

Table 6. Values of $\Delta\epsilon(\lambda_m) \times \phi$ at different monitoring wavelengths (λ_m) from laser flash photolysis of the dyad in THF at excitation wavelengths $\lambda_1 = 450$ nm and $\lambda_2 = 517$ nm.

Excitation wavelength	$\Delta\epsilon(\lambda_m) \times \phi$ ($\text{M}^{-1}\text{cm}^{-1}$)		
	$\lambda_m = 445$ nm	$\lambda_m = 570$ nm	$\lambda_m = 670$ nm
λ_1	10 300	1500	800
λ_2	18 000	2800	1400

porphyrin and flavin moieties are the same, within experimental error, at the three measuring wavelengths. Other transients besides the porphyrin triplet therefore do not contribute to the overall spectrum in a measurable way. In particular, the formation of a sizeable amount of long-lived radical ion species can be ruled out.

Since both the flavin and the porphyrin chromophores contribute to absorption at $\lambda_1 = 450$ nm, two pathways of porphyrin triplet generation must be distinguished at this excitation wavelength. After correction for triplet formation by direct excitation of the porphyrin moiety, a value of $\epsilon(445) \times \phi = 11\,880 \text{ M}^{-1}\text{cm}^{-1}$ was calculated for population of the porphyrin triplet following excitation of the flavin moiety. The ratio of the quantum yields of porphyrin triplet formation upon excitation of one of the two dyad chromophores, $\phi_T(\text{flavin})/\phi_T(\text{porphyrin})$, was therefore determined as 0.66, with an estimated uncertainty margin of $\pm 20\%$. This value is equal, within the error margins, to the corresponding ratio of fluorescence quantum yields (see above).

Conclusions

A strategy for the synthesis of dyads composed of porphyrins and various acceptor moieties using a phenylene and a diazaphenylene spacer has been presented. This method allows the synthesis of similar model compounds from the two building blocks amidine and vinamidinium salt by stepwise addition of pyrimidine rings. The „pyrimidine approach“ in principle is suitable for the synthesis of biomimetic model compounds with well-defined geometry. Various acceptor groups can be used, and the photophysical and spectroscopic properties of the porphyrin can be changed by the incorporation of metal cations. The spacer absorbs only in the far UV region and thus does not interfere with spectroscopic measurements at longer wavelengths. Three examples are presented and the properties of a dyad composed of a porphyrin coupled to a flavin moiety were examined in detailed theoretical and experimental studies.

Semiempirical investigations showed that the distance between the donor and acceptor moieties is fixed but that their relative orientation varies within rather large margins as the activation barrier for rotation about some of the connecting single bonds is low. In the optimum geometry, the orbitals of the spacer moiety are highly conjugated. Essentially, they do not combine with the highest occupied orbitals of the porphyrin subunit but contribute in an important way to those of the flavin subunit. The lowest excited orbitals are strongly centered on the donor and

acceptor subunits. Excitations correlating with those of the porphyrin moiety are thus not greatly changed in the dyad. The lowest flavin excited state shifts to higher energies but its dipole moment is considerably increased and this accounts for strong solvent stabilization of this state, which is therefore found at lower energy and well separated from the porphyrin Soret bands.

A charge-transfer excited state is found at high energies with a large formal dipole moment of >70 D. It results formally from a transfer of an electron from the highest occupied porphyrin orbital to that of the flavin moiety after excitation of the flavin. As the ground-state orbitals are highly delocalized, this could facilitate excited-state charge transfer. In a polar solvent, the energy of the charge-separated state decreases; an estimation of solvent effects places it in the vicinity of the fluorescent porphyrin Q bands. This is in agreement with cyclovoltammetric results which locate this state below the fluorescent state in energy, too. Electron transfer induced by excitation of the flavin subgroup should therefore have a high driving force and could thus be very efficient; the lowest excited state of the porphyrin could also relax to the charge-separated state.

The results of the spectroscopic and photophysical investigations are consistent with this picture. The specific excitations of the subunits are recovered in the spectrum of the dyad in the right order. The flavin moiety can be selectively excited at wavelengths in between the porphyrin Q and Soret bands. Excitation of the dyad always generates the typical porphyrin fluorescence with its characteristic lifetime. The fluorescence quantum yield is slightly higher when the porphyrin moiety is primarily excited; no additional relaxation pathway can be detected in this case. In low and medium polarity solvents (toluene and tetrahydrofuran, but not dimethylformamide) the fluorescence quantum yield depends on the excitation wavelength: it is considerably smaller upon excitation into the flavin moiety. In these cases, relaxation to the fluorescent porphyrin state occurs most probably by intramolecular energy-transfer mechanisms with a yield of the order of 60%. This result is consistent with those of transient absorption measurements which show a decrease of the triplet quantum yields similar to those of the fluorescence yields. In the latter measurements no long-lived transient in the nanosecond time domain could be observed besides the porphyrin triplet–triplet absorption.

Taken together, the results of the theoretical and experimental investigations on the dyad **1a** suggest that a charge-separated state can be populated after excitation of the flavin moiety, which relaxes to the ground state on the subnanosecond time scale. The proposed relaxation scheme is shown in Scheme 4. The experimentally observed solvent dependence is in qualitative agreement with the predictions of the Marcus electron-transfer theory,^[31] yielding a maximum rate of electron transfer at an intermediate value of solvent polarity. The results described in this study demonstrate the interest of this new class of donor–spacer–acceptor compounds for spectroscopic and photophysical investigations. Further work involving variation of the bridge size and structure as well as different donor/acceptor combinations is under way.

Experimental Section

General methods: ^1H NMR spectra were recorded on a Bruker ARX300 (300 MHz) or a Bruker AMX600 (600 MHz) with TMS as internal standard. Infrared spectra were obtained on a Perkin–Elmer FT-IR Spectrum 1000. Electron ionization (EI, 70 eV), fast-atom bombardment (FAB, 20 kV caesium, NBA matrix) and high-resolution (HRMS) mass spectral analyses were performed by Finnigan MAT 95Q. Preparative column chromatography was carried out on glass columns packed with silica gel 60 (Merck, grain size 0.040–0.063 mm). Air-sensitive reactions were carried out under nitrogen in dried solvents and glassware.

6-(4-Ethoxycarbonylmethylanylino)-3-methyluracil (5): 6-Chloro-3-methyluracil^[32] (25.1 g, 156 mmol) and 4-aminophenylacetic acid^[33] (28.0 g, 156 mmol) was added to a mixture of *N,N*-diethylaniline (100 mL) and acetic acid (10 mL) and heated to 190 °C for 25 min. After cooling to room temperature, ethanol (500 mL) was added and the colorless solid was collected by filtration; yield: 39.3 g (83 %). M.p. 274–275 °C; ^1H NMR (300 MHz, $[\text{D}_6]\text{DMSO}$): δ = 1.18 (t, 3J = 7.0 Hz, 3H, CH_2CH_3), 3.06 (s, 3H, NCH_3), 3.60 (s, 2H, CH_2), 4.05 (q, 3J = 7.0 Hz, 2H, CH_2CH_3), 4.79 (s, 1H, uracil H5), 7.09 (d, 3J = 8.0 Hz, 2H, phenyl H2,6), 7.23 (d, 3J = 8.0 Hz, 2H, phenyl H3,5), 8.16 (s, 1H, NH); IR (KBr): $\tilde{\nu}$ = 3259 cm^{-1} , 3099, 2982, 1732, 1625, 1610, 1580, 1299; UV/Vis (DMSO): λ_{max} (lg ϵ) = 288 nm (4.26); $\text{C}_{13}\text{H}_{13}\text{N}_3\text{O}_4$ (275.3): calcd C 56.72, H 4.76, N 15.27; found C 57.08, H 4.90, N 15.24.

10-(4-Ethoxycarbonylmethylphenyl)-3-methylflavin (6a): Compound **5** (18.8 g, 62.0 mmol) and nitrosobenzene (20.0 g, 187 mmol) were refluxed in a mixture of acetic anhydride (100 mL) and acetic acid (25 mL) for 30 min. The solvent was removed in vacuo and the residue was triturated in ethanol (500 mL). After filtration the solid was recrystallized from acetic acid; yield 17.9 g (74 %), orange crystals. M.p. > 300 °C; ^1H NMR (300 MHz, $[\text{D}]\text{TFA}$): δ = 1.46 (t, 3J = 7.0 Hz, 3H, CH_2CH_3), 3.73 (s, 3H, NCH_3), 4.11 (s, 2H, CH_2), 4.53 (q, 3J = 7.1 Hz, 2H, CH_2CH_3), 7.50 (d, 3J = 8.1 Hz, 1H, flavinyl H9), 7.68 (d, 3J = 8.1 Hz, 2H, phenyl H3,5), 7.96 (d, 3J = 8.1 Hz, 2H, phenyl H2,6), 8.25 (t, 3J = 7.8 Hz, 1H, flavinyl H7), 8.32 (t, 3J = 7.9 Hz, 1H, flavinyl H8), 8.65 (d, 3J = 8.3 Hz, 1H, flavinyl H6); IR (KBr): $\tilde{\nu}$ = 3060 cm^{-1} , 2981, 1660, 1616, 1556, 1485, 1318, 1172, 806, 769; UV/Vis (DMSO): λ_{max} (lg ϵ) = 439 nm (3.90), 341 (4.10), 269 (4.44); $\text{C}_{21}\text{H}_{18}\text{N}_4\text{O}_4$ (390.4): calcd C 64.61, H 4.65, N 14.35; found C 64.40, H 4.79, N 14.41.

10-(4-Carboxymethylphenyl)-3-methylflavin (6b): The solution of **6a** (4.0 g, 10.2 mmol) in conc. HCl (350 mL) was stirred at room temperature for 16 h. The solution was diluted with water (600 mL) and the precipitate was collected by filtration. Recrystallization from acetic acid/ethanol gave yellow microcrystals; yield: 2.6 g (72 %). M.p. > 300 °C; ^1H NMR (300 MHz, $[\text{D}]\text{TFA}$): δ = 3.73 (s, 3H, NCH_3), 4.11 (s, 2H, CH_2), 7.50 (d, 3J = 8.0 Hz, 1H, flavinyl H9), 7.68 (d, 3J = 8.0 Hz, 2H, phenyl H3,5), 7.96 (d, 3J = 8.0 Hz, 2H, phenyl H2,6), 8.26 (t, 3J = 7.8 Hz, 1H, flavinyl H7), 8.32 (t, 3J = 7.9 Hz, 1H, flavinyl H8), 8.65 (d, 3J = 8.3 Hz, 1H, flavinyl H6); IR (KBr): $\tilde{\nu}$ = 3068 cm^{-1} , 2964, 1712, 1658, 1616, 1553, 1487, 1281, 1173, 986, 807, 768; UV/Vis (DMSO): λ_{max} : 439 nm, 337, 268; $\text{C}_{19}\text{H}_{14}\text{N}_4\text{O}_4$ (362.3): calcd C 62.98, H 3.89, N 15.46; found C 63.14, H 4.05, N 15.32.

3-Dimethylamino-*N,N*-dimethyl-2-(4-(3-methylflavin-10-yl)-phenyl)-prop-2-eniminium perchlorate (4): A solution of **6b** in DMF (0.7 mL) was added to a solution of the Vilsmeier reagent (prepared by addition of phosphoryl chloride (2.8 g, 18 mmol) to DMF (2.17 g, 30 mmol) at 0 °C and stirring the mixture at room temperature for 1.5 h) and heated to 80 °C for 22 h. After careful addition of water (1.4 mL), a 20 % aqueous solution of sodium perchlorate (10 mL) was added. The precipitate was filtered off and washed with water. Recrystallization from acetonitrile/ether gave yellow microcrystals; yield: 2.7 g (92 %). M.p. > 300 °C. ^1H NMR (300 MHz, $[\text{D}]\text{TFA}$): δ = 2.95 (s, 6H, vinamidinium NCH_3), 3.47 (s, 6H, vinamidinium NCH_3), 3.72 (s, 3H, flavinyl NCH_3), 7.25 (d, 3J = 8.0 Hz, 1H, flavinyl H9), 7.67 (s, 2H, vinamidinium H1,3), 7.89–7.92 (m, 4H, phenyl H2,3,5,6), 8.21–8.26 (m, 2H, flavinyl H7,8), 8.65 (d, 3J = 8.3 Hz, 1H, flavinyl H6); IR (KBr): $\tilde{\nu}$ = 3068 cm^{-1} , 2935, 1710, 1662, 1616, 1591, 1556, 1487, 1400, 1291, 1274, 1122, 1109, 982, 809; UV/Vis (DMSO): λ_{max} : 439 nm, 316, 269; $\text{C}_{24}\text{H}_{25}\text{ClN}_6\text{O}_6$ (529.0) calcd C 54.50, H 4.76, N 15.89; found C 54.33, H 4.89, N 15.77.

3-Methyl-10-(2'-methyl-4,5'-1',3'-diazabiphenyl)-flavin (8): A suspension of **4** (1.85 g, 3.50) and acetamidinium chloride (0.34 g, 3.60 mmol) in pyridine (120 mL) was heated for 22 h. After cooling to room temperature, water (200 mL) was added and the mixture was concentrated to about 100 mL in

vacuo. The precipitate was collected by filtration and washed with hot acetonitrile; yield: 0.97 g (70 %), yellow solid. M.p. > 300 °C. ^1H NMR (300 MHz, $[\text{D}]\text{TFA}$): δ = 3.28 (s, 3H, 2'- CH_3), 3.77 (s, 3H, NCH_3), 7.48 (d, 3J = 8.6 Hz, 1H, flavinyl H9), 8.04 (d, 3J = 8.5 Hz, 2H, H2,6), 8.29 (t, 3J = 7.8 Hz, 1H, flavinyl H7), 8.35 (t, 3J = 7.9 Hz, 1H, flavinyl H8), 8.42 (d, 3J = 8.3 Hz, 2H, H3,5), 8.69 (d, 3J = 8.3 Hz, 1H, flavinyl H6), 9.75 (s, 2H, pyrimidinyl H); MS (EI): m/z 395 [M^+]; IR (KBr): $\tilde{\nu}$ = 1715 cm^{-1} , 1666, 1617, 1589, 1553, 1449, 1276, 984, 806; UV/Vis (DMSO): λ_{max} : 266 nm, 334, 440; $\text{C}_{22}\text{H}_{16}\text{N}_6\text{O}_2 \cdot 0.5 \text{H}_2\text{O}$ (405.4): calcd C 65.18, H 4.23, N 20.73; found C 65.25, H 4.27, N 21.04.

4-(10,15,20-Tris(*p*-tert-butylphenyl)porphyrin-5-yl)-benzonitrile (2): Pyrrole (32 mL, 460 mmol) was added dropwise to a solution of *p*-cyanobenzaldehyde (15 g, 110 mmol) and *p*-tert-butylbenzaldehyde (58 mL, 350 mmol) in refluxing propionic acid (1.7 L). The mixture was refluxed for 1 h and then concentrated to about 200 mL. After cooling to room temperature, it was filtered to isolate the precipitate, which was washed with methanol and chromatographed with chloroform/hexane 2:1 on silica gel. The first fraction was 5,10,15,20-tetrakis(*tert*-butylphenyl)porphyrin; the second fraction was the blue–violet product **2**; yield: 5.2 g (5.6 %) after recrystallization from chloroform/methanol. M.p. > 300 °C; ^1H NMR (300 MHz, CDCl_3): δ = –2.73 (s, 2H, NH), 1.61 (s, 27H, $\text{C}(\text{CH}_3)_3$), 7.76 (d, 3J = 8.2 Hz, 6H, *t*Bu-phenyl H3,5), 8.04 (d, 3J = 7.9 Hz, 2H, phenyl H2,6), 8.13 (d, 3J = 8.2 Hz, 6H, *t*Bu-phenyl H2,6), 8.34 (d, 3J = 7.9 Hz, 2H, phenyl H3,5), 8.69 (d, 3J = 4.7 Hz, 2H, porphyrinyl H2,8), 8.88 (s, 4H, porphyrinyl H12,13,17,18), 8.91 (d, 3J = 4.7 Hz, 2H, porphyrinyl H3,7); MS (EI): m/z (%) 807 [M^+] (100); IR (KBr): $\tilde{\nu}$ = 2962 cm^{-1} , 2230, 1629, 1474, 1108, 968, 801; UV/Vis (CHCl_3): λ_{max} (lg ϵ) = 421 nm (5.63), 518 (4.23), 554 (3.98), 592 (3.73), 648 (3.68); $\text{C}_{57}\text{H}_{53}\text{N}_5$ (808.1): calcd C 84.72, H 6.61, N 8.67; found C 84.76, H 6.50, N 8.73.

10,15,20-Tris(*p*-tert-butylphenyl)-5-(4'-(3-methylflavin-10-yl)-1',3'-diazaza-4,2':5',1''-terphenyl)-porphyrin (1a): A slurry of **2** (750 mg, 0.93 mmol) and lithium bis(trimethylsilyl)amide (790 mg, 4.7 mmol) in dry THF (65 mL) was stirred at room temperature for 51 d. The solvent was removed in vacuo. Toluene (65 mL) and chlorotrimethylsilane (0.67 mL, 5.3 mmol) were added, and the mixture was refluxed for 8 h. The solvent was distilled off and ethanol (45 mL), **4** (2.1 g, 4.0 mmol), KF (580 mg, 10 mmol) and *N*-ethyl-diisopropylamine (0.75 mL, 8.20 mmol) were added. The mixture was stirred at room temperature for 2 d and then refluxed for 2 d. The solvent was removed in vacuo and the residue was washed with water, dried, and chromatographed on silica gel with chloroform/methanol 40:1. The second fraction containing **1a** was isolated as a violet solid; yield: 305 mg (28 %) after recrystallization from chloroform/methanol. M.p. > 300 °C; ^1H NMR (600 MHz, CDCl_3): δ = –2.72 (s, 2H, NH), 1.61 (s, 27H, $\text{C}(\text{CH}_3)_3$), 3.54 (s, 3H, N-CH_3), 7.05 (d, 3J = 8.6 Hz, 1H, flavinyl H9), 7.53 (d, 3J = 8.3 Hz, 2H, phenyl H3',5''), 7.63 (dd, 3J (H7, H6) = 3J (H7, H8) = 7.7 Hz, 1H, flavinyl H7), 7.73 (dd, 3J (H8, H7) = 3J (H8, H9) = 7.7 Hz, 1H, flavinyl H8), 7.76 (d, 3J = 8.2 Hz, 6H, *t*Bu-phenyl H3,5), 8.01 (d, 3J = 8.3 Hz, 2H, phenyl H2'',6''), 8.15 (d, 3J = 8.2 Hz, 6H, *t*Bu-phenyl H2,6), 8.39–8.42 (m, 3H, phenyl H2,6, flavinyl H6), 8.87–8.93 (m, 10H, porphyrinyl H, phenyl H3,5), 9.27 (s, 2H, pyrimidinyl H); IR (KBr): $\tilde{\nu}$ = 2961 cm^{-1} , 1671, 1556, 1432, 967, 801; UV/Vis (CHCl_3): λ_{max} (lg ϵ) = 272 nm (4.80), 421 (5.70), 518 (4.29), 554 (4.10), 593 (3.77), 649 (3.77); HRMS (EI): calcd for $\text{C}_{77}\text{H}_{66}\text{N}_{10}\text{O}_2$ 1162.5370, found 1162.5376; $\text{C}_{77}\text{H}_{66}\text{N}_{10}\text{O}_2$ (1163.4): calcd C 79.49, H 5.72, N 12.04; found C 79.15, H 5.84, N 11.83.

[10,15,20-Tris(*p*-tert-butylphenyl)-5-(4'-(3-methylflavin-10-yl)-1',3'-diazaza-4,2':5',1''-terphenyl)porphyrinato]zinc(II) (1b): Zinc acetate dihydrate (100 mg, 0.46 mmol) was added to a suspension of **1a** (130 mg, 0.11 mmol) in DMF (15 mL). The mixture was refluxed for 30 min and then diluted with water (30 mL). The residue was filtered off, washed with water, and chromatographed on silica gel with chloroform/methanol 30:1 to give a red–violet solid; yield: 98 mg (71 %). M.p. > 300 °C; ^1H NMR (600 MHz, CDCl_3): δ = 1.61 (s, 27H, $\text{C}(\text{CH}_3)_3$), 3.53 (s, 3H, N-CH_3), 7.04 (d, 3J = 8.2 Hz, 1H, flavinyl H9), 7.52 (d, 3J = 8.1 Hz, 2H, phenyl H3',5''), 7.63 (dd, 3J (H7, H6) = 3J (H7, H8) = 8.2 Hz, 1H, flavinyl H7), 7.73 (dd, 3J (H8, H7) = 3J (H8, H9) = 8.2 Hz, 1H, flavinyl H8), 7.75 (d, 3J = 8.0 Hz, 6H, *t*Bu-phenyl H3,5), 8.01 (d, 3J = 8.1 Hz, 2H, phenyl H2'',6''), 8.14 (d, 3J = 8.0 Hz, 6H, *t*Bu-phenyl H2,6), 8.38 (d, 3J = 8.2 Hz, 1H, flavinyl H6), 8.41 (d, 3J = 8.0 Hz, 2H, phenyl H2,6), 8.90 (d, 3J = 8.0 Hz, 2H, phenyl H3,5), 8.96–9.00 (m, 8H, porphyrinyl H), 9.26 (s, 2H, pyrimidinyl H); IR (KBr): $\tilde{\nu}$ = 2961 cm^{-1} , 1673, 1556, 1432, 999, 798; UV/Vis (CHCl_3): λ_{max} (lg ϵ) = 272 nm (4.79), 422 (5.75), 550 (4.38), 589 (3.86); HRMS (EI): calcd for

$C_{77}H_{64}N_{10}O_2Zn$ 1224.4505, found 1224.4615; $C_{77}H_{64}N_{10}O_2Zn \cdot 1.5H_2O$ (1253.8): calcd C 73.76, H 5.39, N 11.17; found C 74.03, H 5.59, N 10.96.

10,15,20-tris(*p*-*tert*-butylphenyl)porphyrin-5-(4-(5-Cyanopyrimidin-2-yl)-phenyl) (10): A slurry of **2** (600 mg, 0.74 mmol) and lithium bis(trimethylsilyl)amide (1.12 mg, 6.7 mmol) in dry THF (25 mL) was stirred at room temperature for 5 d. The solvent was removed in vacuo. Toluene (25 mL) and chlorotrimethylsilane (0.88 mL, 6.9 mmol) were added, and the mixture was refluxed for 8 h. The solvent was distilled off and **9**^[24] (1.71 g, 6.80 mmol), KF (1.4 mg, 24 mmol), and pyridine (20 mL) were added. The mixture was heated under reflux for 2 d. The solvent was removed in vacuo and the residue was washed with water, dried, and chromatographed on silica gel with chloroform. The second fraction containing **10** was isolated as a violet solid; yield: 480 mg (73 %). M.p. > 300 °C. ¹H NMR (300 MHz, CDCl₃): δ = −2.73 (s, 2H, NH), 1.60 (s, 27H, C(CH₃)₃), 7.75 (d, ³*J* = 7.9 Hz, 6H, *t*Bu-phenyl H3,5), 8.14 (d, ³*J* = 7.9 Hz, 6H, *t*Bu-phenyl H2,6), 8.40 (d, ³*J* = 8.2 Hz, 2H, phenyl H2,6), 8.84–8.93 (m, 10H, porphyrinyl H, phenyl H3,5), 9.17 (s, 2H, pyrimidinyl H); MS (EI): *m/z* (%) 885 [*M*⁺] (100); IR (KBr): $\tilde{\nu}$ = 2961 cm^{−1}, 2231, 1577, 1429, 967, 801; UV/Vis (CHCl₃): λ_{max} (lg ϵ) = 293 nm (4.46), 422 (5.55), 520 (4.25), 556 (4.09), 593 (3.80), 649 (3.79); C₆₄H₅₃N₇ (886.2): calcd C 82.68, H 6.26, N 11.07; found C 82.68, H 6.43, N 10.90.

10,15,20-Tris(*p*-*tert*-butylphenyl)-5-(4'''-(3-methylflavin-10-yl)-1',1'',3',3''-tetraaza-4,2':5',1'':5'',1'''-quaterphenyl)porphyrin (1c): A slurry of **10** (350 mg, 0.40 mmol) and lithium bis(trimethylsilyl)amide (330 mg, 1.97 mmol) in dry THF (25 mL) was stirred at room temperature for 5 d. The solvent was removed in vacuo. Toluene (25 mL) and chlorotrimethylsilane (0.30 mL, 2.4 mmol) were added, and the mixture was refluxed for 8 h. The solvent was distilled off and ethanol (20 mL), **4** (850 mg, 1.6 mmol), KF (230 mg, 4.0 mmol), and *N*-ethyl-diisopropylamine (0.60 mL, 3.4 mmol) were added. The mixture was stirred at room temperature for 2 d and then refluxed for 2 d. The solvent was removed in vacuo and the residue was filtered off, washed with water, dried, and chromatographed on silica gel with chloroform/methanol 20:1 (2nd fraction). The fraction was concentrated and **1c** was covered with a threefold amount of methanol to give a violet solid; yield: 38 mg (7.8 %). M.p. > 300 °C; ¹H NMR (600 MHz, CDCl₃): δ = −2.72 (s, 2H, NH), 1.61 (s, 27H, C(CH₃)₃), 3.53 (s, 3H, N-CH₃), 7.02 (d, ³*J* = 7.6 Hz, 1H, flavinyl H9), 7.52 (d, ³*J* = 8.6 Hz, 2H, phenyl H3''', 5'''), 7.63 (dd, ³*J* (H7,H6) = ³*J* (H7, H8) = 7.6 Hz, 1H, flavinyl H7), 7.73 (dd, ³*J* (H8,H7) = ³*J* (H8, H9) = 7.6 Hz, 1H, flavinyl H8), 7.76 (d, ³*J* = 8.1 Hz, 6H, *t*Bu-phenyl H3,5), 7.97 (d, ³*J* = 8.2 Hz, 2H, phenyl H2'', 6''), 8.15 (d, ³*J* = 8.1 Hz, 6H, *t*Bu-phenyl H2,6), 8.38–8.42 (m, 3H, phenyl H2,6, flavinyl H6), 8.87–8.90 (m, 8H, porphyrinyl H), 8.96 (d, ³*J* = 8.0 Hz, 2H, phenyl H3,5), 9.22 (s, 2H, pyrimidinyl' H), 10.00 (s, 2H, pyrimidinyl' H); IR (KBr): $\tilde{\nu}$ = 2961 cm^{−1}, 1674, 1556, 1413, 967, 802; UV/Vis (CHCl₃): λ_{max} (lg ϵ) = 272 nm (4.66), 421 (5.62), 518 (4.08), 554 (3.77), 592 (3.51), 648 (3.50); MS (EI): *m/z* 1240 [*M*⁺]; HRMS (EI): calcd for C₈₁H₆₈N₁₂O₂ 1240.5588, found 1240.5702; C₈₁H₆₈N₁₂O₂ · 1 H₂O (1258.2): calcd C 77.24, H 5.60, N 13.34; found C 77.08, H 5.81, N 12.92.

Computational methods: Quantum mechanical calculations of the electronic properties of the dyad in the ground and excited states were carried out with version 6.1 of the program package VAMP^[34] using the AM1 Hamiltonian.^[35] A detailed study of the ground-state structure has been published previously.^[25] Excited states were obtained from a configuration interaction scheme including all single and pairwise double excitations (AM1/PECI)^[36] within an active space of 12 orbitals, that is, including all molecular orbitals in between HOMO − 5 and LUMO + 5. This yields 109 configurations. All calculations were performed for the geometry of the electronic ground state as given in ref. [25]. No electron correlation is taken into account for the ground-state optimizations. The molecular properties were visualized by the program TRAMP, version 1.1.^[37] All calculations were performed on SGI INDY workstations (MIPS R4400).

Optical spectroscopy: Infrared spectra were obtained on a Perkin–Elmer FT-IR Spectrometer 1000. Electronic absorption spectra were recorded on a Hitachi U-3300 UV/Vis spectrometer; corrected fluorescence spectra were obtained with a luminescence spectrometer LS 50 B (Perkin–Elmer). The fluorescence quantum yields were determined relative to *meso*-tetraphenylporphyrin (*Q_F* = 0.09 in *n*-propanol) and acridinin yellow (*Q_F* = 0.5 in ethanol). Time-correlated single photon counting was used to obtain fluorescence decay profiles with a Model 5000 W fluorescence lifetime spectrometer with the SAFE option from IBH Consultants,

Edinburgh (Scotland). For determination of the porphyrin fluorescence lifetime the apparatus was equipped with a special red-sensitive photomultiplier tube (type 3237, Hamamatsu, Japan). The deconvolution procedure was described elsewhere.^[38–40]

The solvents toluene, tetrahydrofuran, and *N,N*-dimethylformamide were of the highest available purity and were checked for impurities by absorption and fluorescence spectroscopy.

Laser flash photolysis: A broadband optical parametric oscillator (Lamdba-Physik OPPO) pumped by the third harmonic of a Nd:YAG laser (Coherent Infinity) was used as the excitation source in transient absorption spectroscopy. This setup delivered pulses with a duration (FWHM) of about 3 ns and a spectral bandwidth of the order of 10 cm^{−1} in the wavelength region of interest (450–520 nm); pulse-to-pulse reproducibility was of the order of 20 %. Time-resolved absorbance was measured in a right-angle geometry as described earlier.^[41] In this setup, both exciting and analysing light beams are delimited by rectangular apertures which define a reaction volume of dimensions 0.17 cm (height) and 0.32 cm by 0.13 cm (width and depth, respectively, as seen from the laser beam) at the entrance of the sample cell. The pulse energy delivered to the sample was varied between 0.02 and 1 mJ/pulse by adjusting the pumping level and measured at the sample cell location using a ballistic calorimeter (Raycon-WEC 730). Transient absorption data, each measurement representing the average of 30–100 individual pulses, were taken as a function of exciting pulse energy; values of $\Delta\epsilon(\lambda_m) \times \phi$, where $\Delta\epsilon(\lambda_m)$ is the laser-induced change of extinction coefficient at the measuring wavelength and ϕ the photoprocess quantum yield, are extracted from these data provided the plot of transient absorbance vs. pulse energy is linear, representing a one-photon process.

Acknowledgments

S.S., A.P., G.G., and G.K. thank the Fonds zur Förderung der wissenschaftlichen Forschung in Österreich for financial support (Project NR. P11880-CHE).

- a) V. Balzani, F. Scandola, *Supramolecular Photochemistry*; Ellis Horwood, Chichester, **1991**, p. 161–196, 355–394; b) D. Gust, *Nature* **1997**, 386, 21; c) S. Speiser, *Chem. Rev.* **1996**, 96, 1953.
- a) J. Deisenhofer, H. Michel, *Angew. Chem.* **1989**, 101, 872; *Angew. Chem. Int. Ed. Engl.* **1989**, 28, 829; b) R. Huber, *Angew. Chem.* **1989**, 101, 849; *Angew. Chem. Int. Ed. Engl.* **1989**, 28, 848.
- a) M. R. Wasielewski, *Chem. Rev.* **1992**, 34, 435; b) H. Kurreck, M. Huber, *Angew. Chem.* **1995**, 107, 929; *Angew. Chem. Int. Ed. Engl.* **1995**, 34, 849; c) D. Gust, T. A. Moore, *Top. Curr. Chem.* **1991**, 159, 103–151; d) D. Gust, T. A. Moore, A. L. Moore, *Acc. Chem. Res.* **1993**, 26, 198; e) M. Bixon, J. Fajer, G. Feher, J. H. Freed, D. A. Gamliel, A. J. Hoff, H. Levanon, K. Möbius, R. Nechushtai, J. R. Norris, A. Scherz, J. L. Sessler, D. Stehlik, *Isr. J. Chem.* **1992**, 32, 469.
- a) D. Gust, T. A. Moore, *Science* **1989**, 244, 35; b) V. Balzani, F. Scandola, *Supramolecular Photochemistry*, Ellis Horwood, Chichester, **1991**, p. 110–122.
- a) R. W. Wagner, J. S. Lindsey, *J. Am. Chem. Soc.* **1994**, 116, 9759; b) R. W. Wagner, T. E. Johnson, J. S. Lindsey, *J. Am. Chem. Soc.* **1996**, 118, 11166; c) J. S. Hsiao, B. P. Krueger, R. W. Wagner, T. E. Johnson, J. K. Delaney, D. C. Mauzerall, G. R. Fleming, J. S. Lindsey, D. F. Bocian, R. J. Donohoe, *J. Am. Chem. Soc.* **1996**, 118, 11181; d) F. Li, S. I. Yang, Y. Ciringh, J. Seth, C. H. Martin, D. L. Singh, D. Kim, R. R. Birge, D. F. Bocian, D. Holtz, J. S. Lindsey, *J. Am. Chem. Soc.* **1998**, 120, 10001; e) A. Osuka, K. Maruyama, I. Yamazaki, N. Tamai, *Chem. Phys. Lett.* **1990**, 165, 392; f) A. L. Moore, G. Dirks, D. Gust, T. A. Moore, *Photochem. Photobiol.* **1980**, 32, 691.
- a) H. Dieks, J. Sobek, P. Tian, H. Kurreck, *Tetrahedron Lett.* **1992**, 33, 5951; b) J. von Gersdorff, B. Kirste, H. Kurreck, *Liebigs Ann. Chem.* **1993**, 897; c) L. Sun, J. von Gersdorff, J. Sobek, H. Kurreck, *Tetrahedron* **1995**, 51, 3535; d) M. Fuchs, J. von Gersdorff, H. Dieks, H. Kurreck, K. Möbius, T. Prisner, *J. Chem. Soc. Faraday Trans.* **1996**, 92, 949; e) H. Dieks, M. O. Senge, B. Kirste, H. Kurreck, *J. Org. Chem.* **1997**, 62, 8666; f) H. Szelinski, D. Niethammer, P. Tian, H. Kurreck,

- Tetrahedron* **1996**, 52, 8497; g) K. A. Jolliffe, T. D. M. Bell, K. P. Ghiggino, S. J. Langford, M. N. Paddon-Row, *Angew. Chem.* **1998**, 110, 960; *Angew. Chem. Int. Ed.* **1998**, 37, 916; h) H. A. Staab, R. Hauck, B. Popp, *Eur. J. Org. Chem.* **1998**, 631; i) M. S. Vollmer, F. Effenberger, T. Stümpfling, A. Hartschuh, H. Port, H. C. Wolf, *J. Org. Chem.* **1998**, 63, 631.
- [7] a) F. Effenberger, H. Schlosser, P. Bäuerle, S. Maier, H. Port, H. C. Wolf, *Angew. Chem.* **1988**, 100, 274, *Angew. Chem. Int. Ed. Engl.* **1988**, 27, 281; b) F. Effenberger, *New J. Chem.* **1991**, 15, 117; c) N. Hell, H. Port, H. C. Wolf, H. Strobel, F. Effenberger, *Chem. Phys.* **1993**, 176, 215; d) B. Heine, E. Sigmund, H. Port, *J. Mol. Electronics* **1991**, 7, 29; e) A. G. Hyslop, M. J. Therien, *Inorg. Chim. Acta* **1998**, 275–276, 427.
- [8] a) M. S. Vollmer, F. Würthner, F. Effenberger, P. Emele, D. U. Meyer, T. Stümpfig, H. Port, H. C. Wolf, *Chem. Eur. J.* **1998**, 4, 260; b) F. Würthner, M. S. Vollmer, F. Effenberger, P. Emele, D. U. Meyer, H. Port, H. C. Wolf, *J. Am. Chem. Soc.* **1995**, 117, 8090; c) P. Emele, D. U. Meyer, N. Holl, H. Port, H. C. Wolf, F. Würthner, P. Bäuerle, F. Effenberger, *Chem. Phys.* **1994**, 181, 417; G. Hungerford, M. van der Auwerder, J.-C. Chambron, V. Heitz, J.-P. Sauvage, J.-L. Pierre, D. Zurita, *Chem. Eur. J.* **1999**, 5, 2089.
- [9] a) R. Gompper, H.-J. Mair, K. Polborn, *Synthesis* **1997**, 696; b) R. Gompper, *J. Prakt. Chem.* **1994**, 336, 390; c) S. Brandl, R. Gompper, K. Polborn, *J. Prakt. Chem.* **1996**, 338, 451; d) R. Gompper, C. Harfmann, K. Polborn, *J. Prakt. Chem.* **1998**, 340, 381.
- [10] The term is used in different ways. According to F. Müller, *Top. Curr. Chem.* **1983**, 108, 71, the flavin unit carries two methyl groups in positions C-7 and C-8; the unsubstituted compound is named isoalloxazine. According to H. Beyer, W. Walter, *Lehrbuch der Organischen Chemie*, 21st ed., Thieme, Stuttgart, **1988**, p. 802, the name “flavin” is used for both compounds.
- [11] C. J. Walker, T. W. Griffiths, *FEBS Lett.* **1988**, 239, 259.
- [12] a) S. Fukuzumi, T. Tanaka in *Photoinduced Electron Transfer* (Eds.: M. A. Fox, M. Chanan), Elsevier, Amsterdam, **1988**, part C, p. 636; b) C. Walsh, *Acc. Chem. Res.* **1980**, 13, 148; c) T. C. Bruice, *Acc. Chem. Res.* **1980**, 13, 256.
- [13] V. d. Bergh-Snorek, M. T. Stankovich, *J. Am. Chem. Soc.* **1984**, 106, 3685.
- [14] a) J. Takeda, S. Ohta, M. Hirobe, *J. Am. Chem. Soc.* **1987**, 109, 7677; b) P. Nayar, A. M. Brun, A. Harriman, T. P. Begley, *J. Chem. Soc. Chem. Commun.* **1992**, 395; c) K. Hasharoni, H. Levanon, J. Gätschmann, H. Schubert, H. Kurreck, K. Möbius, *J. Phys. Chem.* **1995**, 99, 7514.
- [15] J. H. Wang, *Acc. Chem. Res.* **1970**, 3, 90.
- [16] a) D. Lloyd, H. McNab, *Angew. Chem.* **1976**, 88, 496; *Angew. Chem. Int. Ed. Engl.* **1976**, 15, 459; b) R. M. Wagner, C. Jutz, *Chem. Ber.* **1971**, 104, 2975; c) H. Zeschke, S. Arndt, V. Wagner, H. Schubert, *Z. Chem.* **1977**, 17, 293.
- [17] a) A. D. Adler, F. R. Longo, J. D. Finarelli, J. Goldmacher, J. Assour, L. Korsakoff, *J. Org. Chem.* **1967**, 32, 476; b) D. G. Neilson in *The Chemistry of Amidines and Imidates* (Eds.: S. Patai, Z. Rappoport), Wiley, Chichester, **1991**, p. 425.
- [18] a) A. R. Sanger, *Inorg. Nucl. Chem. Lett.* **1973**, 9, 351; b) A. W. Cordes, R. C. Haddon, R. G. Hicks, R. T. Oackley, T. T. M. Palstra, L. F. Schneemeyer, J. V. Waszczak, *J. Am. Chem. Soc.* **1992**, 114, 5000; R. T. Boere, R. T. Oackley, R. W. Reed, *J. Organomet. Chem.* **1987**, 331, 161.
- [19] A. D. Adler, F. R. Longo, F. Kampas, J. Kim, *J. Inorg. Nucl. Chem.* **1970**, 32, 2443.
- [20] F. Yoneda, K. Shinozuka, K. Tsukuda, A. Koshiro, *J. Heterocyclic Chem.* **1979**, 16, 1365.
- [21] A. C. Schnock, Ph.D. Thesis, Universität München, **1995**.
- [22] Crystal data for **4**: C₂₄H₂₅ClN₆O₆, *M*_r = 528.95, orthorhombic, space group *Pbca*, *a* = 1192.5(4), *b* = 1513.0(5), *c* = 2728.2(7) pm, *Z* = 8, *V* = 4922(3), ρ_{calcd} = 1.428 g cm⁻³, μ = 0.208 mm⁻¹. Data collection: NON-IUS CAD4 diffractometer, ω -scan, scan width (0.55 + 0.35 tan θ)° crystal dimensions 0.17 × 0.47 × 0.67, maximum measuring time 90 s, graphite monochromated MoK α radiation (λ = 0.71073 Å). 3405 measured, 3404 independent reflections, 2740 classed observed (*I* > 2 σ *I*); refined parameters: 339. Solution of structure: SIR92, refinement with SHELXL93. Final *R*1 = 0.0525 and *wR*2 = 0.1566 for *I* > 2 σ *I* and *R*1 = 0.0657 and *wR*2 = 0.1648 for all data; largest/smallest residual density 0.617/–0.270 e Å⁻³. Crystallographic data (excluding structure factors) for the structure reported in this paper have been deposited with the Cambridge Crystallographic Data Centre as supplementary publication no. CCDC-115670. Copies of the data can be obtained free of charge on application to CCDC, 12 Union Road, Cambridge CB2 1EZ, UK (fax: (+44) 1223-336-033; e-mail: deposit@ccdc.cam.ac.uk).
- [23] a) D. Lloyd, H. McNab, *Angew. Chem.* **1976**, 88, 496; b) B. W. Matthews, R. E. Stenkamp, P. M. Colman, *Acta Crystallogr.* **1973**, B 29, 449.
- [24] J. Kucera, Z. Arnold, *Coll. Czech. Chem. Commun.* **1967**, 32, 1704.
- [25] A. Parusel, *J. Mol. Model.* **1998**, 4, 366.
- [26] M. Gouterman, G. H. Wagniere, L. C. Snyder, *J. Mol. Spectrosc.* **1963**, 11, 108.
- [27] C. J. F. Böttcher, In *Theory of electric polarisation*, Vol. I., Elsevier, Amsterdam, **1973**, p. 153.
- [28] D. Majumdar, R. Sen, K. Bhattacharyya, S. P. Bhattacharyya, *J. Phys. Chem.* **1991**, 95, 4324.
- [29] M. Gouterman, In *The Porphyrins*, Vol. III, Physical Chemistry, Part B (Ed.: D. Dolphin), Academic Press, NY, **1978**, p. 1.
- [30] a) C. El Hanine-Lmoumene, L. Lindqvist, *Photochem. Photobiol.* **1997**, 66, 591; b) I. Carmichael, G. L. Hug, *J. Phys. Chem. Ref. Data* **1986**, 15, 1.
- [31] a) R. A. Marcus, *J. Chem. Phys.* **1989**, 93, 3078; b) I. R. Gould, S. Farid, R. H. Young, *J. Photochem. Photobiol. A* **1992**, 65, 133; c) G. Köhler, K. Rechthaler, G. Grabner, R. Lubodradzki, K. Suwinska, K. Rotkiewicz, *J. Phys. Chem. A* **1997**, 101, 8518.
- [32] G. Nübel, W. Pfeleiderer, *Chem. Ber.* **1962**, 95, 1605.
- [33] H. Salkowski, *Chem. Ber.* **1895**, 28, 1917.
- [34] G. Rauhut, A. Alex, J. Chandrasekhar, T. Steinke, W. Sauer, B. Beck, M. Hutter, P. Gedeck, T. Clark, *VAMP6.1*, Oxford Molecular, Oxford, **1997**.
- [35] M. J. S. Dewar, E. G. Zoebisch, E. F. Healy, J. J. P. Stewart, *J. Am. Chem. Soc.* **1985**, 107, 3402.
- [36] T. Clark, J. Chandrasekhar, *Isr. J. Chem.* **1993**, 33, 435.
- [37] H. Lanig, R. König, T. Clark, *TRAMPI.1b*, Erlangen, **1995**.
- [38] G. Köhler, *J. Photochem.* **1986**, 35, 189.
- [39] G. Köhler, K. Rotkiewicz, *Spectrochim. Acta* **1986**, A 42, 1127.
- [40] G. Köhler, P. Wolschann, *J. Chem. Soc. Faraday Trans. II*, **1987**, 83, 513.
- [41] G. Grabner, N. Getoff, T. Gantchev, D. Angelov, M. Shopova, *Photochem. Photobiol.* **1991**, 54, 673.

Received: February 26, 1999 [F1638]